energies

MDPI

Article

Maximum Power Point Tracking Technology of Photovoltaic Array under Partial Shading Based On Adaptive Improved Differential Evolution Algorithm

Peng Zhang and Huibin Sui *

Key Laboratory of Power System Intelligent Dispatch and Control of Ministry of Education, Shandong University, Jinan 250061, China; 201834400@mail.sdu.edu.cn

* Correspondence: suihuibin@sdu.edu.cn

Received: 4 February 2020; Accepted: 5 March 2020; Published: 8 March 2020

Abstract: In the case of partial shading conditions, there will be more than one maximum power point (MPP) in photovoltaic (PV) array. The traditional maximum power point tracking (MPPT) methods are easy to get in the local maximum power point (LMPP) and fail. Based on the standard differential evolution (DE) algorithm, the mutation strategy, scaling factor F, and cross factor CR of the algorithm are optimized. Also, the population position variance δ^2 is used to prevent falling into LMPP. Finally, the conditions for algorithm termination and restart are set. It is verified by simulation that the method has fast convergence speed, high accuracy, and can adapt well to changes in the external environment. The improved DE algorithm has a great advantage in MPPT.

Keywords: MPPT; differential evolution algorithm; photovoltaic array; DC-DC converter

1. Introduction

Energy is not only the driving force of economic development but also the power of automation and modernization. Renewable energy has developed rapidly in recent years. Solar energy is one of the renewable energy sources that does not produce any carbon dioxide, solid or liquid waste, and has obvious environmental advantages compared with other energy sources [1]. PV power generation system is a system that converts the inexhaustible solar energy into electric energy, but it has a high dependence on the environmental conditions, especially most affected by the light. One of the ways to improve the efficiency of PV power generation is MPPT control [2].

Traditional MPPT methods, such as constant voltage method, perturbation and observation method (P&O), incremental conductance method (INC), hill climbing method (HC), among others, are effective when the light conditions are constant. However, when the PV array is under partial shading conditions (PSC), there will be more than one maximum power point. The traditional tracking method is easy to get in the LMPP and cannot accurately track the global maximum power point (GMPP) [3,4], which leads to PV array output power loss. Many scholars have proposed the MPPT methods for PV array under PSC. In references [5,6] the particle swarm optimization (PSO) algorithm is proposed to track the GMPP. This method simulates the foraging process of birds to search for the best power point, having the advantages of fast convergence speed and high efficiency. However, PSO is prone to premature convergence and falls into LMPP, resulting in low convergence accuracy. In reference [7], sliding mode variable structure control is used to track the MPP under irregular shadow, which has the advantages of fast control speed and strong robustness. However, when the state trajectory reaches the sliding surface, it is difficult to slide strictly along the sliding surface toward the balance point, but to cross back and forth on both sides of the sliding surface, resulting in vibration and power loss. In references [8–10], fuzzy control is used for MPPT, which does not require an accurate mathematical

model and has strong robustness. However, it is difficult to establish a fuzzy rule because it needs to accumulate a lot of operation experience of power point tracking. In references [11,12], neural networks are used to track the MPP. This method also requires the distribution of power extremum points under many different shadows, so it is not practical. In references [13,14], Fibonacci is used to track the GMPP; this method also depends on the learning to the peak distribution, and it is easy to fall into LMPP. Reference [15] proposed a dichotomy, the first step is to find the vicinity of GMPP, and the second step is to use traditional MPPT method to track MPPs, but the dichotomy will fail in the case of complex shading. Reference [16] proposed a MPPT method using shading detection and the trend of slopes from each section of the curve. After the short-term and long-term testing, this method shows the advantages of high precision and short tracking time. In reference [17] a modified P&O MPPT algorithm is proposed for accurate detection of PSC, which stabilizes the system output voltage without compromising the power efficiency. Reference [18] proposed an algorithm that is based on bio-inspired Whale Optimization. This algorithm eliminates the computational burden faced by the hybrid MPPT algorithms as discussed in various references and reduces the power oscillation during the change in operating conditions. Reference [19] proposed a modified P&O MPPT that can be used under PSC effectively, by integrating the Artificial Bee Colony algorithm in the first stage and P&O algorithm in the second stage. However, the algorithm needs many parameters to be adjusted, which is not conducive to control.

Based on the advantages and disadvantages of the above methods, the DE algorithm is used to optimize the output of PV array. DE only needs two adjustable parameters. Firstly, according to the method proposed in reference [20], the initial positions of particles are selected near the voltages corresponding to the possible MPPs to avoid falling into the LMPP. The mutation direction, mutation operator, and crossover operator of particles are optimized based on the traditional DE algorithm.

2. PV System Characteristics and Models

2.1. Characteristics Analysis of PV Module

PV modules use the PV effect of semiconductor materials to convert solar energy into electrical energy. A PV module is a large PN junction. When the sunlight hit on the PV module surface, free charges in the battery start to move, and different potential differences occur in different parts, thus forming current. According to the electronic circuit theory, the equivalent circuit diagram and output characteristic equation of PV modules can be obtained [21,22]. The equivalent circuit diagram is shown in Figure 1.

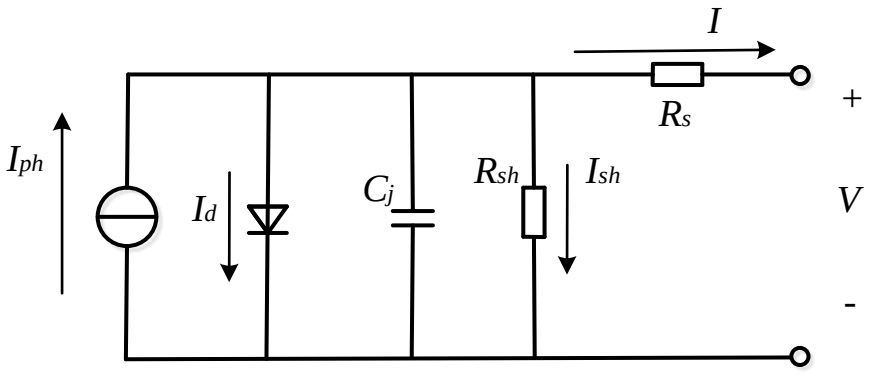

Figure 1. Photovoltaic (PV) module equivalent circuit.

When the light intensity of the external sunlight remains unchanged, so does the PV module's photocurrent. At this time, the PV module can be equivalent to a constant current source. Generally, the output current of PV module is hardly affected by the junction capacitance C_j, so

the effect of C_j can be ignored in the equivalent circuit of PV module. The *I-V* characteristic equation of PV the module is derived as follows:

$$I = I_{ph} - I_d - I_{sh} \tag{1}$$

$$I_d = I_0\left\{\exp\left[\frac{q(V+IR_s)}{AkT}\right]-1\right\} \tag{2}$$

$$I = I_{ph} - I_0\left\{\exp\left[\frac{q(V+IR_s)}{AkT}\right]-1\right\} - \frac{V+IR_S}{R_{sh}} \tag{3}$$

$$I_{sc} = I_0\left[\exp\left(\frac{qV_{oc}}{AkT}\right)-1\right] \tag{4}$$

$$V_{oc} = \frac{AkT}{q}ln\left(\frac{I_{sc}}{I_0}+1\right) \tag{5}$$

where I is the output current of the PV module; I_{ph} is photocurrent; I_d is diode junction current; I_{sh} is diode leakage current; I_0 is diode reverse saturation current; I_{sc} is short-circuit current of PV module; V_{oc} is open circuit voltage of PV module; A is ideal factor of PN junction; R_s is series resistance; R_{sh} is parallel resistance; q is the amount of charge contained in a single electron; k is Boltzmann constant; T on behalf of the temperature (°F).

In the actual equivalent circuit, the resistance value of parallel resistance R_{sh} is very large. As such, the term $(V + IR_s)/R_{sh}$ can be ignored in Equation (3), thus Equation (6) is obtained, which is the *I-V* characteristic equation of PV modules.

$$I = I_{ph} - I_0\left\{\exp\left[\frac{q(V+IR_s)}{AkT}\right]-1\right\} \tag{6}$$

Assuming that the output voltage of the PV module is V, the output power P is represented as Equation (7):

$$P = VI = VI_{ph} - VI_0\left\{\exp\left[\frac{q(V+IR_s)}{AkT}\right]-1\right\} \tag{7}$$

The PV module model is established with Matlab/Siumlink, simulation parameters are set as follows: V_{oc} = 22.2 V, I_{sc} = 8.58 A, V_m = 17.7 V, I_m = 7.94 A. The I-V and P-V curves under different light intensity S and temperature T are shown in Figures 2 and 3.

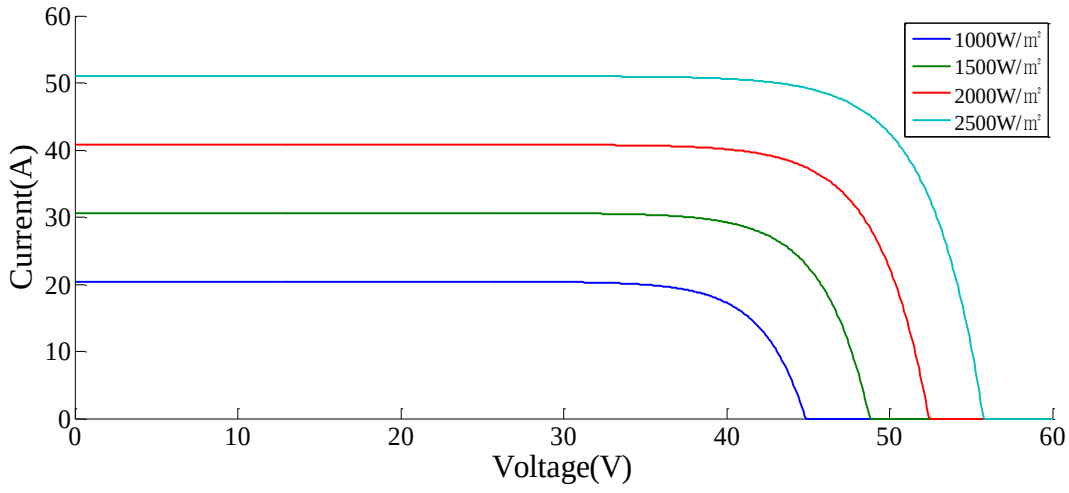

(**a**)

Figure 2. *Cont.*

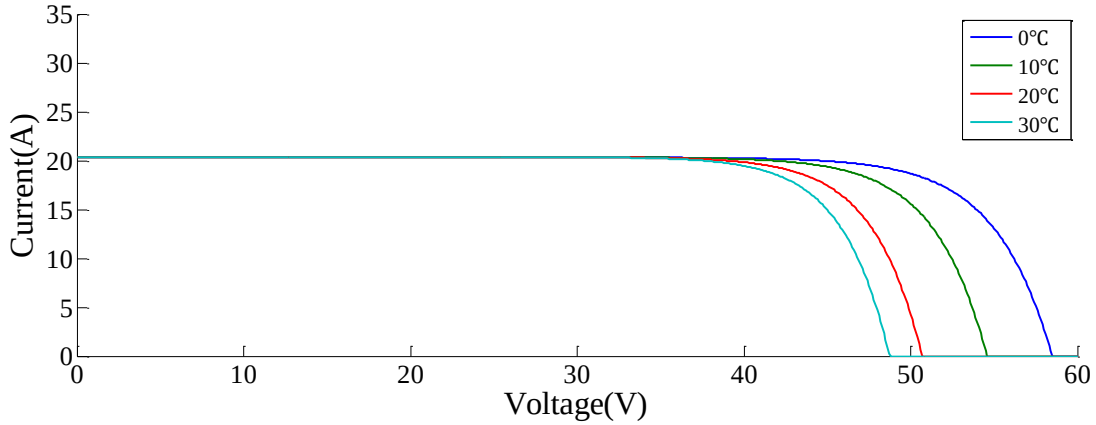

(**b**)

Figure 2. I-V output characteristics of PV modules in different environments. (**a**) I-V output characteristics of PV modules under different light intensity at T = 25 °C. (**b**) I-V output characteristics of PV modules under different temperatures at S = 1000 W/m^2.

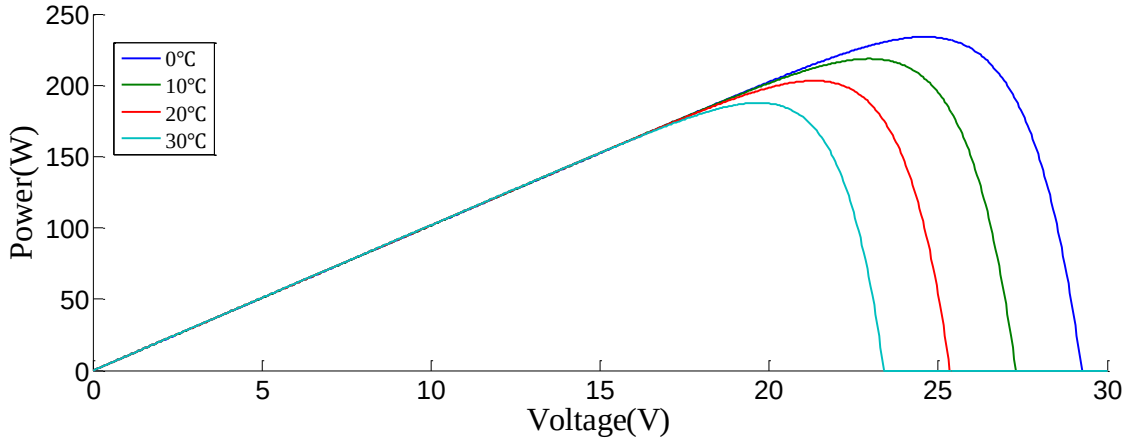

(**a**)

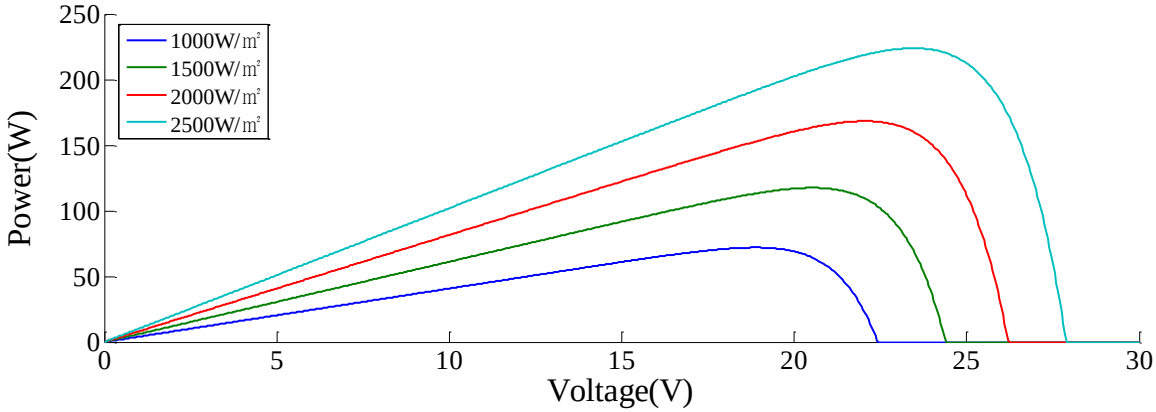

(**b**)

Figure 3. P-V output characteristics of PV modules in different environments. (**a**) P-V output characteristics of PV modules under different temperatures at S = 1000 W/m^2 (**b**) P-V output characteristics of PV modules under different light intensity at T = 25 °C.

The curves show that the light intensity is the main factor affecting the output specific properties of PV modules.

2.2. Characteristic Analysis of PV Array

The PV array is composed of PV modules in series and parallel. The output power of the PV array is the sum of each PV module, while in the case of PSC, the output power of each series branch is different. Under this condition, the output power is mismatched in the whole PV system, resulting in "hot spot effect". To reduce the harm of "hot spot effect" on PV modules, a bypass diode needs to be directly paralleled at the positive and negative poles of each PV module [23]. Figure 4 shows a 4 × 3 PV array.

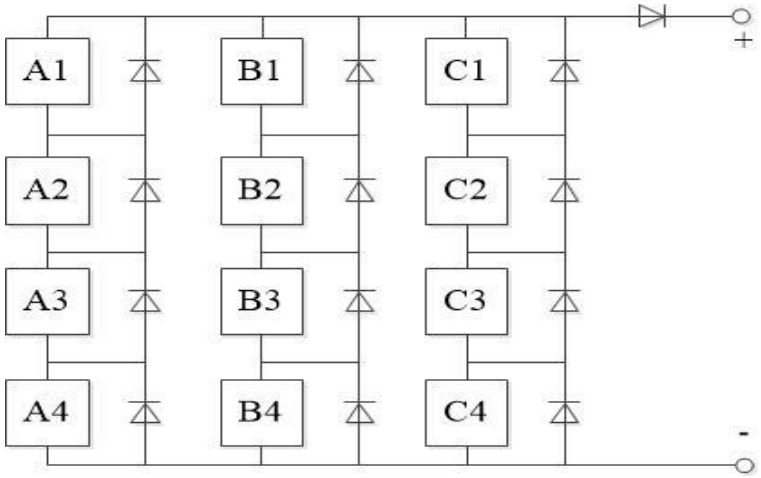

Figure 4. Structure of 4 × 3 PV array.

According to the reference [20], in the case of different shading conditions in each group, there are n + 1 MPPs in the m × n PV array. The array voltage corresponding to the n peak points is about $l \times 0.8\ Voc\_module$, l = 1~n − 1; the (n + 1)th peak point is approximately $0.85\ Voc\_array$. In this paper, two different shadow conditions are set up, under the environmental temperature of 25 °C. The first case is [3:2:1]: A2 = 800 W/m^2, A3 = 700 W/m^2, A4 = 500 W/m^2; B3 = 620 W/m^2, B4 = 350 W/m^2; C4 = 600 W/m^2. The second case is [3:2:0]: A2 = 800 W/m^2, A3 = 500 W/m^2, A4 = 400 W/m^2; B3 = 700 W/m^2, B4 = 400 W/m^2. The output characteristics of the PV array are shown in Figures 5 and 6.

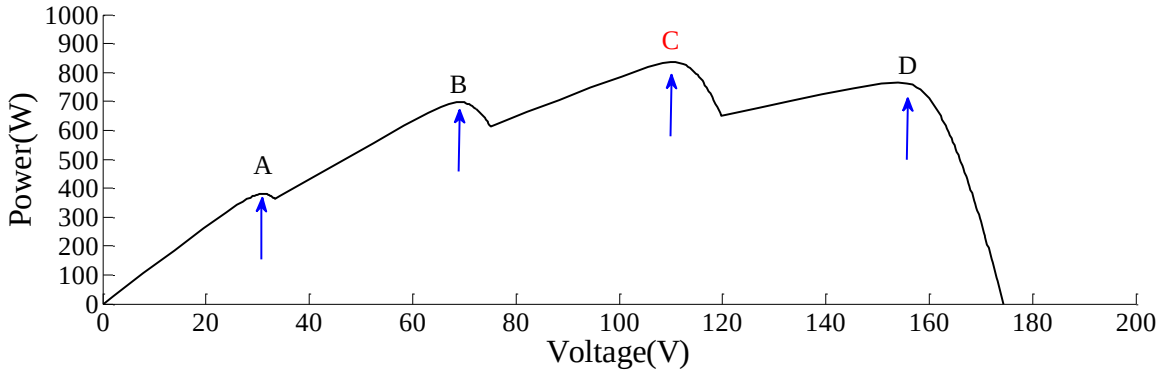

Figure 5. P-V curve of PV array under the first shade condition.

In Figure 5, points A, B, and D are LMPPs, point C is GMPP; in Figure 6, points A and B are LMPPs, point C is GMPP, and the distribution of MPPs meets the positions proposed in reference [20]. Therefore, to avoid getting in LMPPs, the selection of initial voltage values is particularly important.

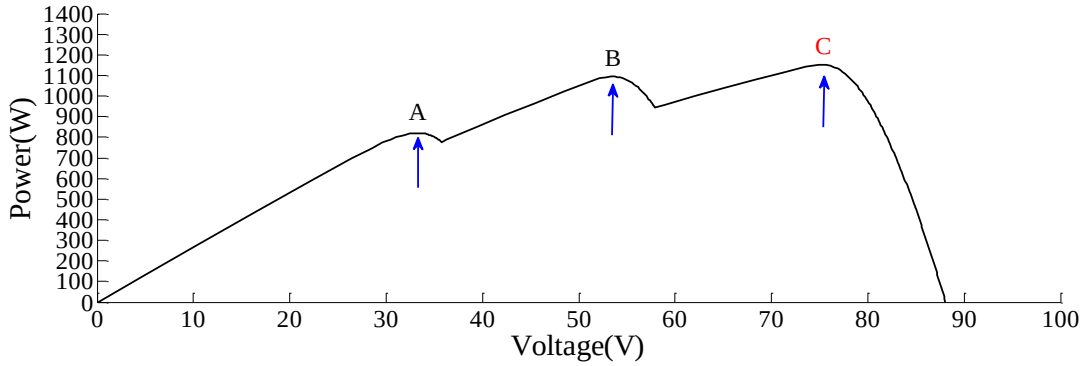

Figure 6. P-V curve of PV array under the second shade condition.

2.3. DC-DC Converter

There are many types of common DC chopper circuits. The boost chopper circuit and the buck chopper circuit are the two most basic types. The efficiency of the boost circuit is higher than buck circuit. As long as the input inductance is large enough, the input current can be continuous and very smooth; also, the electromagnetic interference to the power side is relatively small. Then the boost circuit is chosen as the voltage adjustment circuit in the research. The schematic diagram is shown in Figure 7.

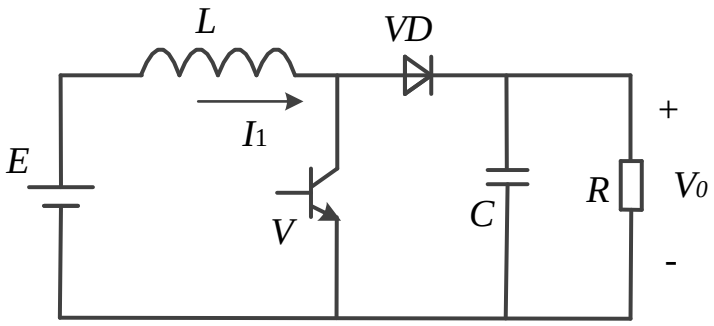

Figure 7. Boost chopper circuit.

When switch V is on, power supply E charges inductor L with charging current I_1. At the same time, capacitor C supplies power to the load R. Because the value of C is very large, the output voltage V_0 is constant. When the switch V is on, the energy accumulated on the inductance L is $E\ I_1 t_{on}$. When switch V is off, the energy released by inductance L is $(V_0 - E)\ I_1 t_{off}$. In steady state, the energy stored and released by inductance L is equal in a period T, as shown in Equation (8):

$$EI_1 t_{on} = (V_0 - E) I_1 t_{off} \tag{8}$$

It can be simplified to:

$$V_0 = \frac{t_{on} + t_{off}}{t_{off}} E = \frac{T}{t_{off}} E \tag{9}$$

The output voltage is always higher than the supply voltage, therefore this circuit is called a boost chopper circuit, also known as a boost converter.

3. Standard DE Algorithm and Proposed Adaptive DE MTTP Algorithm

3.1. Standard DE Algorithm

The DE algorithm was first proposed by Storm and Price in 1995, it is an optimization algorithm based on swarm intelligence theory. Cooperation and competition among individuals in a group guide

the optimization search. DE has the characteristics of high efficiency, good convergence, and strong robustness. Moreover, it has a unique memory ability to dynamically track the current search situation, that makes it simple and practical, achieving good results in many fields [24]. The standard DE algorithm mainly includes four steps: initialization, mutation, crossover and selection, as shown in Figure 8.

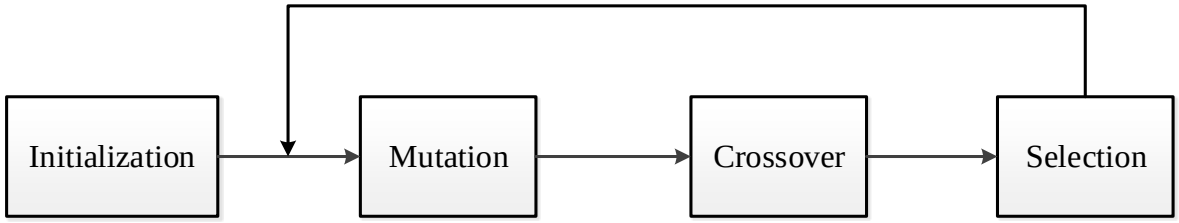

Figure 8. Schematic diagram of differential evolution (DE) algorithm.

3.1.1. Initialization

The first step of the DE algorithm is particle swarm optimization. Considering D-dimensional real space S⊂RD as the search space of optimization problem. The first population $P_1 = \{X_1^1, \ldots \ldots, X_{NP}^1\}$ parallel search in searching space, which consists of *NP* D-dimensional real parameter vectors $X_1^t = \{X_{i1}^t, X_{i2}^t, \ldots \ldots, X_{iD}^t\} \in S$ ($i = 1, \ldots \ldots, NP$). The initial particles are required to be distributed uniformly throughout the whole searching range. X_{ij} is calculated using Equation (10):

$$X_{ij} = L_j + rand(0,1) * \left(U_j - L_j\right) \quad i = 1, 2, \ldots, NP; j = 1, 2, \ldots, \tag{10}$$

where *rand* (0,1) generates a random number between 0 and 1; $[L_j, U_j]$ represents the value range of dimension *j*.

3.1.2. Mutation

Biologically, the mutation is a sudden change in the genetic characteristics of chromosomes. In the DE algorithm, the simplest form of mutation is randomly select three different parameter vectors X_{r1}^t, X_{r2}^t, X_{r3}^t from the current population. Taking any two of the three vectors to subtract, multiply the difference by *F* and add the remained vector to get the third vector. So that the mutation vector $V_i^t = (V_{i1}^t, \ldots \ldots, V_{iD}^t)$ is obtained, as shown in Equation (11):

$$V_i^t = X_{r1}^t + F \cdot \left(X_{r2}^t - X_{r3}^t\right) \tag{11}$$

In the Equation (11), the subscripts *r*1, *r*2, and *r*3 are mutually different integers randomly selected from the set {1, 2, ... , *NP*}. These integers are generated randomly for each mutation vector and are different from the current target vector index *i*. For this reason, the population size must meet $NP \geq 4$.

3.1.3. Crossover

To improve the diversity of the population, the DE algorithm also uses cross operation. Crossover refers to the cross operation between the target vector X_i^t and the mutation vector V_i^t to generate a trial vector U_i^t. There are exponential and binomial crossovers. The binomial crossover method is described in Equation (12):

$$U_{ij}^t = \begin{cases} V_{ij}^t, \ rand \leq CR \\ X_{ij}^t, \ otherwise \end{cases} \tag{12}$$

where *CR* is a crossover factor, *rand* is a random number between [0, 1]. At least one mutation vector is introduced into the trial vector.

3.1.4. Selection

The DE adopts a greedy selection strategy, which competes the trial vector U_i^t with the target vector X_i^t to determine which vector will enter to the next generation. Equation (13) shows the calculation for X_i^{t+1}:

$$X_i^{t+1} = \begin{cases} U_i^t, f\left(U_i^t\right) \le f\left(X_i^t\right) \\ X_i^t, \ otherwise \end{cases} \tag{13}$$

if the fitness of the trial vector *f(U)* is less than or equal to the target vector *f(X)*, the trial vector will replace the target vector into the next generation, otherwise, the target vector will remain unchanged [25–27].

3.2. Proposed Adaptive Improved DE Algorithm for Partial Shading MTTP

In the case of PSC, there will be multiple MPPs in the PV array. Therefore, the DE MPPT algorithm takes the output voltage V as the target vector and the output power P as the fitness function. The particle's initial positions are set in the positions mentioned in the first section where MPPs may occur. The following are the proposed improvement strategies.

3.2.1. Optimal Mutation Strategy

In the mutation operation of standard DE/rand/1/bin strategy, the mutated base vector X_{r1}^t is selected from three randomly selected individuals, which is beneficial to the global search but slows down the convergence rate. From the perspective of vector calculation, vectors have the problem of superposition directions. Searching towards the individual vector with the best fitness makes it easier to find the global optimal solution. Three randomly selected vectors are sorted according to their fitness. The best fitness individual is recorded as X_b^t, the second fitness individual is recorded as X_m^t, and the worst fitness individual is recorded as X_w^t. The new mutation operation is shown in Equation (14):

$$V_i^t = X_b^t + F \cdot \left(X_m^t - X_w^t\right) \tag{14}$$

Thus, the modified mutation operation is no longer a completely random search, but a search in the direction of the basis vector X_b^t. The three vectors of each mutation are randomly selected, so this is a kind of certainty in random, which can guarantee the global search performance of the algorithm. The generation diagram of the mutation vector is shown in Figure 9.

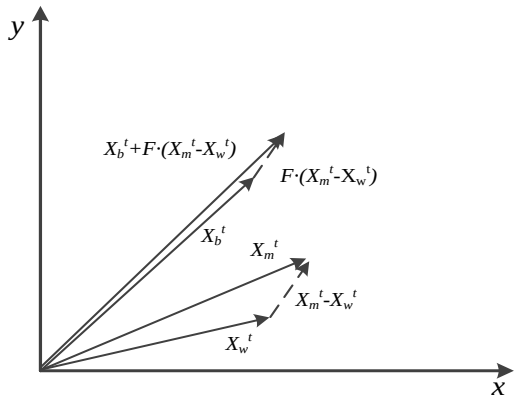

Figure 9. Generation diagram of two-dimensional function mutation vector.

3.2.2. Adaptive Control Strategy of Scaling Factor *F*

F controls scaling disturbance of the base vector. A larger *F* value is good for global search, but not good for the convergence in the later search period. On the contrary, local search is fast, but it is easy to

fall into LMPP. To maintain population diversity and strengthens local search ability the value of F is changed according to the iteration times, as shown in Equation (15):

$$F = F_l + F_h \cdot \frac{G_{max} - G}{G_{max}} \tag{15}$$

where F_l = 0.1, F_h = 0.8, G_{max} is the maximum iteration number, and G is the current iteration number. Therefore, F takes a larger value at the beginning of the iteration, which is conducive to global search. As the iteration progresses, the F decreases continuously to rapidly converge to improve efficiency.

3.2.3. Adaptive Strategy of Cross Factor *CR*

According to the binomial cross Equation (12), if the CR becomes larger, the mutation vector V_i^t contributes more to the trial vector U_i^t. It is beneficial to local search and accelerates convergence rate, however, it leads more damage to the target vectors which have better fitness. Otherwise, if the CR becomes smaller, the target vector X_i^t contributes more to the trial vector U_i^t. The smaller CR is beneficial to maintain population diversity and global search performance, but it is not good for generating new individual structures, that will make the searching process slow. Therefore, the value of CR can be determined according to the Equation (16):

$$CR = \begin{cases} CR_h, \ f\left(U_i^t\right) \geq f\left(X_i^t\right) \\ CR_l, \ f\left(U_i^t\right) < f\left(X_i^t\right) \end{cases} \tag{16}$$

where $CR_h = 0.6, CR_l = 0.4$.

3.2.4. Self-Adaptive Mutation

If the group shows the phenomenon of premature convergence, then the individual's position difference will become smaller and smaller. An adaptive mutation strategy is proposed to prevent the population from falling into LMPP. The group position variance δ^2 is defined as Equation (17):

$$\delta^2 = \sum_{i=1}^{NP} \frac{(X_i - X_{avg})^2}{NP} \tag{17}$$

where X_{avg} represents the average position of particles.

The population position variance reflects the aggregation degree of individuals in the group. The smaller the value of δ^2, the more aggregation degree of the group; otherwise, the more dispersed. When the particles are at the LMPPs, the value of δ^2 will be small, and a threshold value α can be given at this time. If δ^2 is greater than α, the particle positions are relatively scattered, and the mutation is carried out according to the optimal mutation strategy. If δ^2 is less than α, it means that the particles are trapped in the LMPPs or the GMPP. At this time, the variable β is defined. The value of β is determined by the difference between the maximum fitness $f\left(X_i^t\right)$ of the swarm particles and the fitness $f\left(X_{avg}^t\right)$ corresponding to the average position of the particles. If β is greater than constant A, the algorithm falls into LMPPs and reinitialize the group. If β is smaller than A, the group is at the GMPP and outputs the maximum power.

3.2.5. Conditions for Algorithm Termination and Restart

Repeated iterations will result in slow convergence and power fluctuation. When the maximum distance between particles satisfies the Equation (18), it can be considered that all particles gather at the voltage of the GMPP, and the calculation is stopped.

$$|X_{max} - X_{min}| \leq 1\% U_{oc\_array} \tag{18}$$

where U_{oc_array} is open circuit voltage of PV array.

When the shadow or light intensity changes, the output power of the PV array will change, so it is necessary to restart the algorithm for optimization. The conditions for algorithm restart can be determined according to the size of the output current or power of the PV array, as shown in Equation (19):

$$\Delta I = |I - I_{old}| > 0.1 \tag{19}$$

where I is PV array present output current, I_{old} is the last output current.

If the output current of the PV array meets Equation (19), the algorithm should be restarted for a new optimization operation.

The flow chart of proposed adaptive improved DE algorithm is shown in Figure 10.

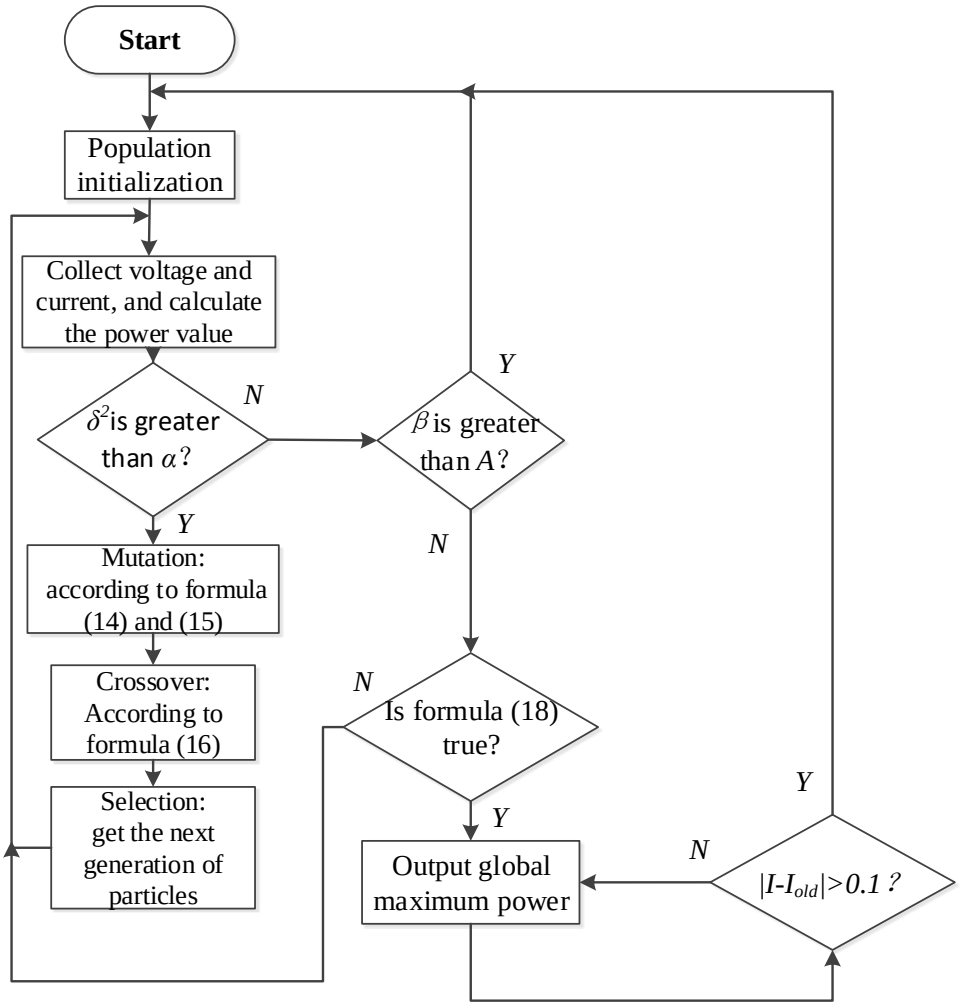

Figure 10. MPPT control flowchart of PV array with improved DE algorithm.

4. Simulation Results

The simulation is established on the Matlab/Simulink simulation platform, as shown in Figure 11. The number of particles is 50, and the maximum number of iterations is 100. The parameters of each component in the simulation are shown in Table 1.

1. In case 1 of shading [3:2:1], the simulation results of the improved DE algorithm, DE algorithm and PSO algorithm are shown in Figure 12.
2. In case 2 of shading [2:1:1], the simulation results of the improved DE algorithm, DE algorithm and PSO algorithm are shown in Figure 13.

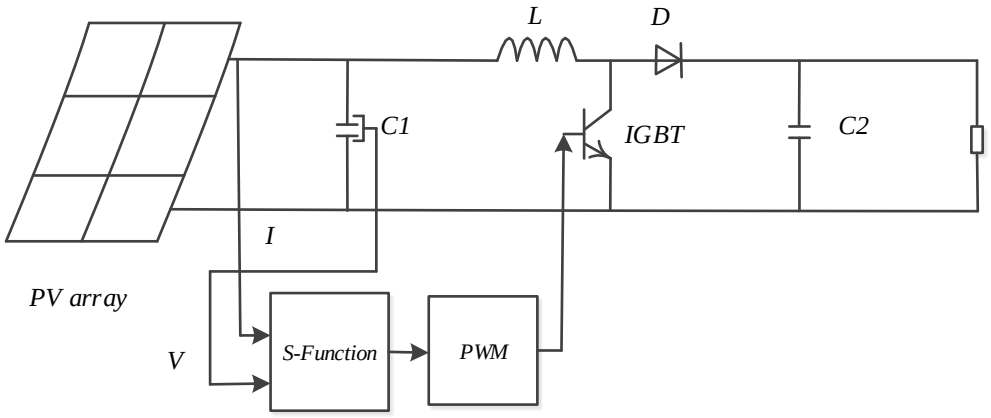

Figure 11. Simulation diagram of PV array.

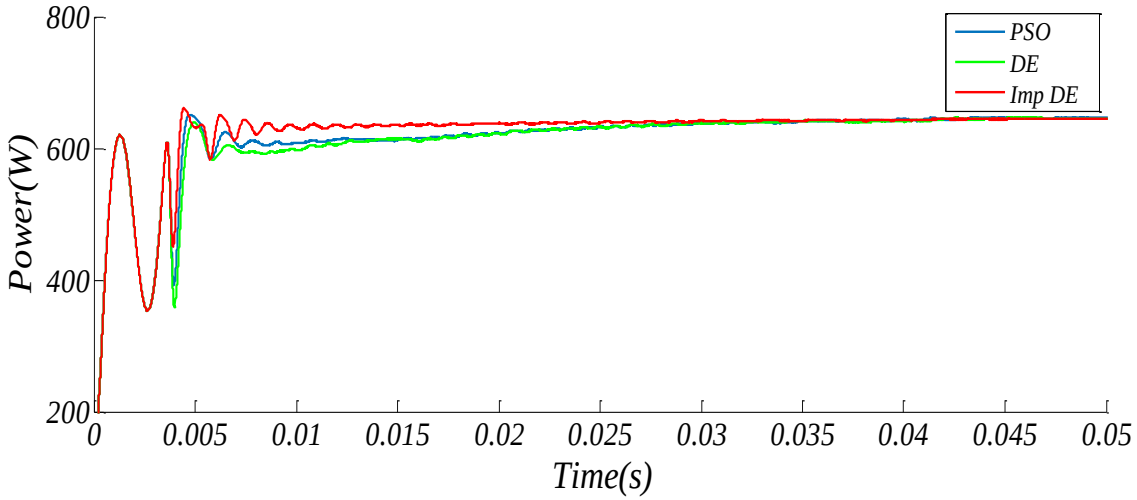

Figure 12. Simulation diagram of particle swarm optimization (PSO), DE algorithm and improved DE algorithm in case 1.

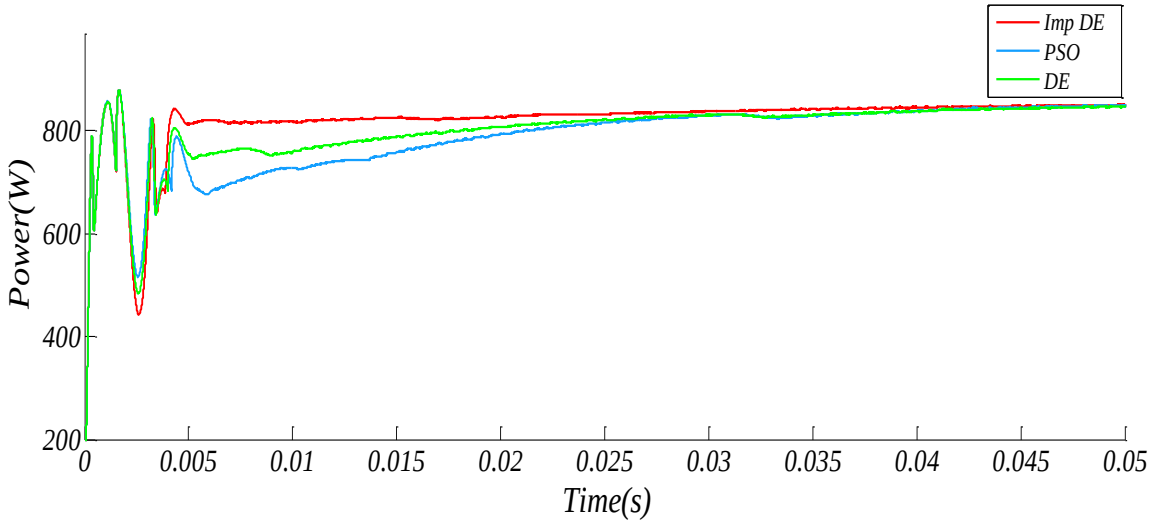

Figure 13. Simulation diagram of PSO, DE algorithm and improved DE algorithm in case 2.

Table 1. Parameters of simulation components.

Components	Parameters
Open circuit voltage of PV module, V_{oc}	43.6 V
Short circuit current of PV module, I_{sc}	8.35 A
Peak power voltage of PV module, V_{mp}	35 V
Peak power current of PV module, I_{mp}	7.6 A
$C1$	50 uF
$C2$	100 uF
L	10 mH
R	50 Ω

As can be seen from the figures above, the improved DE algorithm converges to the GMPP faster than the PSO algorithm and the standard DE algorithm, and will not generate oscillation after stabilization. Table 2 shows the convergence speed, accuracy, and number of iterations to find the GMPP of the three methods in two cases.

Table 2. Comparisons of convergence speed, accuracy and iteration times of the three methods.

	Convergence Time (s)	Steady State Oscillation Loss (W)	Iterations (time)
		Case 1	
PSO	0.035	0.7	46
DE	0.032	0.83	58
Improved DE	0.019	0.3	40
		Case 2	
PSO	0.042	0.8	50
DE	0.039	0.79	56
Improved DE	0.02	0.32	45

According to the calculation equation of MPPT efficiency η proposed in the reference [6], the efficiency of three methods is calculated using Equation (20):

$$\eta = \frac{P_1}{P_2} \times 100\% \tag{20}$$

where P_1 is the steady-state output power of the PV system with the MPPT algorithm. P_2 is the theoretical maximum output power of the PV system under certain PSC. Table 3 shows the MPPT efficiency η of the three methods in two cases.

Table 3. Comparisons of MPPT efficiency of the three methods.

	Case 1			**Case 2**		
	$\mathbf{P_1}$	$\mathbf{P_2}$	$\boldsymbol{\eta}$	$\mathbf{P_1}$	$\mathbf{P_2}$	$\boldsymbol{\eta}$
PSO	644.30 (W)	714.23 (W)	90.20%	856.23 (W)	887.34 (W)	96.49%
DE	645.15 (W)	714.23 (W)	90.33%	855.14 (W)	887.34 (W)	96.37%
Improved DE	644.57 (W)	714.23 (W)	90.24%	857.56 (W)	887.34 (W)	96.64%

From Table 3, it can be seen that the improved DE algorithm has the highest MPPT efficiency under different shading conditions in the three algorithms.

3. When the shading situation changes abruptly, light intensity changes from 1200 W/m^2 to 1000 W/m^2 and finally to 800 W/m^2, Figure 14 shows the output power curve of the improved DE algorithm.

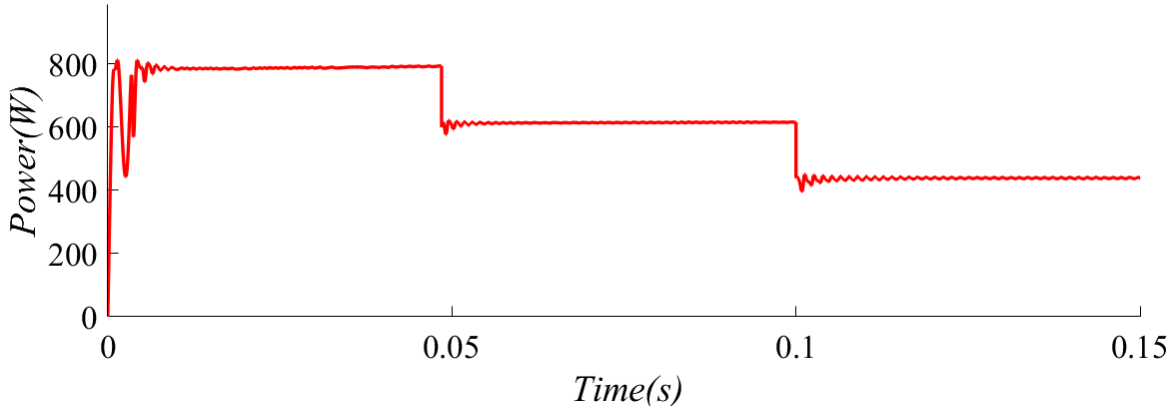

Figure 14. Simulation results when shading situation changes suddenly.

The above simulation results show that the improved DE algorithm has distinct advantages over both the PSO algorithm and the standard DE algorithm in terms of convergence time and steady-state oscillation loss. It can track the new GMPP quickly and accurately under changing shading conditions.

5. Discussion

The traditional MPPT algorithm will fall into a LMPP and cause power loss when the PV array is partially shaded. Compared with other algorithms, the DE algorithm has the advantages of fewer adjustment parameters, fast convergence speed, high accuracy, and strong robustness. Based on the standard DE algorithm, this paper adopts an adaptive DE algorithm with optimal mutation strategy, adaptive scaling factor F and cross factor CR to track the GMPP of PV arrays under PSC. Moreover, the initial positions of the particles were set near the voltage values corresponding to the possible MPPs and using group position variance δ^2 to prevent falling into LMPPs. Finally, conditions are set for algorithm termination and restart.

The improved DE algorithm is an optimization algorithm based on modern intelligence theory, which has a good application prospect. This algorithm can not only be applied to the MPPT of PV array in the shade, but also in data mining, pattern recognition, digital filter design, artificial neural network, electromagnetics and other fields.

6. Conclusions

Based on the standard DE algorithm, this research proposes an improved DE algorithm by studying the output characteristics of PV arrays under partial shading conditions. To track the GMPP of PV arrays, the work presents the optimal mutation strategy, adaptive scaling factor F and the cross factor under PSC by using mathematical equations. Through the simulation with Matlab/Simulink, the result shows that the GMPP tracking process is successful with accuracy. Compared to the PSO and the standard DE algorithm, the proposed algorithm has distinct advantages because it has a higher convergence speed and less steady-state oscillation loss, while fits the required MPPT efficiency.

Author Contributions: P.Z. conceived the methodology, developed the theory, performed the computations, and prepared this paper. H.S. performed the supervision, provided critical feedback, and helped to shape the research. All authors have read and agreed to the published version of the manuscript.

Funding: This research received no external funding.

Conflicts of Interest: The authors declare no conflict of interest.

References

1. Hosenuzzaman, M.; Rahim, N.A.; Selvaraj, J.; Hasanuzzaman, M.; Malek, A.A.; Nahar, A. Global prospects, progress, policies, and environmental impact of solar photovoltaic power generation. *Renew. Sustain. Energy Rev.* **2015**, *41*, 284–297. [CrossRef]
2. Zhao, J.; Zhao, Z.; Zhou, D. Current situation and development of solar photovoltaic power generation technology. *Electr. Appl.* **2007**, *26*, 6–10.
3. Ramyar, A.; Iman-Eini, H.; Farhangi, S. Global Maximum Power Point Tracking Method for Photovoltaic Arrays under Partial Shading Conditions. *IEEE Trans. Ind. Electron.* **2017**, *64*, 2855–2864. [CrossRef]
4. Esram, T.; Chapman, P.L. Comparison of Photovoltaic Array Maximum Power Point Tracking Techniques. *IEEE Trans. Energy Convers.* **2007**, *22*, 439–449. [CrossRef]
5. Ishaque, K.; Salam, Z.; Amjad, M.; Mekhilef, S. An Improved Particle Swarm Optimization (PSO)–Based MPPT for PV With Reduced Steady-State Oscillation. *IEEE Trans. Power Electron.* **2012**, *27*, 3627–3638. [CrossRef]
6. Li, H.; Yang, D.; Su, W.; Lü, J.; Yu, X. An Overall Distribution Particle Swarm Optimization MPPT Algorithm for Photovoltaic System under Partial Shading. *IEEE Trans. Ind. Electron.* **2018**, *66*, 265–275. [CrossRef]
7. Zhou, T.; Sun, W. Maximum power point tracking of photovoltaic array under nonuniform shadow conditions. *Power Syst. Autom.* **2015**, *39*, 42–49.
8. Larbes, C.; Ait Cheikh, S.M.; Obeidi, T.; Zerguerras, A. Genetic Algorithms Optimized Fuzzy Logic Control for the Maximum Power Point Tracking in Photovoltaic System. *Renew. Energy* **2009**, *34*, 2093–2100. [CrossRef]
9. Alajmi, B.N.; Ahmed, K.H.; Finney, S.J.; Williams, B.W. Fuzzy-Logic-Control Approach of a Modified Hill-Climbing Method for Maximum Power Point in Microgrid Standalone Photovoltaic System. *IEEE Trans. Power Electron.* **2010**, *26*, 1022–1030. [CrossRef]
10. Kwan, T.H.; Wu, X. Maximum power point tracking using a variable antecedent fuzzy logic controller. *Sol. Energy* **2016**, *137*, 189–200. [CrossRef]
11. Veerachary, M.; Senjyu, T.; Uezato, K. Neural-network-based maximum-power-point tracking of coupled-inductor interleaved-boost-converter-supplied PV system using fuzzy controller. *IEEE Trans. Ind. Electron.* **2003**, *50*, 749–758. [CrossRef]
12. Lin, F.J.; Lu, K.C.; Yang, B.H. Recurrent Fuzzy Cerebellar Model Articulation Neural Network Based Power Control of Single-Stage Three-Phase Grid-Connected Photovoltaic System During Grid Faults. *IEEE Trans. Ind. Electron.* **2016**, *64*, 1258–1268. [CrossRef]
13. Ramaprabha, R.; Mathur, B.; Ravi, A.; Aventhika, S. Modified Fibonacci Search Based MPPT Scheme for SPVA under Partial Shaded Conditions. In Proceedings of the Third International Conference on Emerging Trends in Engineering and Technology, Goa, India, 19–21 November 2010; IEEE Computer Society: Washington, DC, USA, 2010.
14. Fei, Y.; Jing, H. MPPT for Photovoltaic Generation Based on Fibonacci Numbers Search Control Strategy. *Mod. Electron. Tech.* **2009**, *32*, 182–185.
15. Kobayashi, K.; Takano, I.; Sawada, Y. A study of a two stage maximum power point tracking control of a photovoltaic system under partially shaded insolation conditions. *Sol. Energy Mater. Sol. Cells* **2006**, *90*, 2975–2988. [CrossRef]
16. Gosumbonggot, J.; Fujita, G. Partial Shading Detection and Global Maximum Power Point Tracking Algorithm for Photovoltaic with the Variation of Irradiation and Temperature. *Energies* **2019**, *12*, 202. [CrossRef]
17. Javed, K.; Ashfaq, H.; Singh, R. A new simple MPPT algorithm to track MPP under partial shading for solar photovoltaic systems. *Int. J. Green Energy* **2020**, *17*, 48–61. [CrossRef]
18. Premkumar, M.; Sowmya, R. An effective maximum power point tracker for partially shaded solar photovoltaic systems. *Energy Rep.* **2019**, *5*, 1445–1462. [CrossRef]
19. Pilakkat, D.; Kanthalakshmi, S. An improved P&O algorithm integrated with artificial bee colony for photovoltaic systems under partial shading conditions. *Sol. Energy* **2019**, *178*, 37–47.
20. Zhu, Y.; Shi, X.; Yang, Q.; Li, P.; Liu, W.; Wei, D.; Fu, C. Application of particle swarm optimization algorithm in multi peak maximum power point tracking of photovoltaic array. *Chin. J. Electr. Eng.* **2012**, *32*, 42–48.
21. Vimalarani, C.; Kamaraj, N.; Chitti, B.B. Improved Method of Maximum Power Point Tracking of Photovoltaic (PV) Array using Hybrid Intelligent Controller. *Opt. Int. J. Light Electron Opt.* **2018**, *168*, 403–415.

22. Ashouri-Zadeh, A.; Toulabi, M.; Dobakhshari, A.S.; Taghipour-Broujeni, S.; Ranjbar, A.M. A novel technique to extract the maximum power of photovoltaic array in partial shading conditions. *Int. J. Electr. Power Energy Syst.* **2018**, *101*, 500–512. [CrossRef]
23. Tang, R.-L.; Wu, Z.; Fang, Y.-J. Maximum power point tracking of large-scale photovoltaic array. *Sol. Energy* **2016**, *134*, 503–514. [CrossRef]
24. Liu, B.; Wang, L.; Jin, Y. Research progress of differential evolution algorithm. *Control. Decis.* **2007**, *22*, 3–11.
25. Taheri, H.; Salam, Z.; Ishaque, K. A Novel Maximum Power Point Tracking Control of Photovoltaic System Under Partial and Rapidly Fluctuating Shadow Conditions Using Differential Evolution. In Proceedings of the IEEE Symposium on Industrial Electronics & Applications (ISIEA), Penang, Malaysia, 3–5 October 2010; IEEE: Piscataway, NJ, USA, 2011.
26. Tey, K.S.; Mekhilef, S.; Seyedmahmoudian, M.; Horan, B.; Oo, A.T.; Stojcevski, A. Improved Differential Evolution-based MPPT Algorithm using SEPIC for PV Systems under Partial Shading Conditions and Load Variation. *IEEE Trans. on Ind. Inform.* **2018**, *14*, 4322–4333. [CrossRef]
27. Su, Y.-X.; Chi, R. Multi-objective particle swarm-differential evolution algorithm. *Neural Comput. Appl.* **2017**, *28*, 407–418. [CrossRef]

© 2020 by the authors. Licensee MDPI, Basel, Switzerland. This article is an open access article distributed under the terms and conditions of the Creative Commons Attribution (CC BY) license (http://creativecommons.org/licenses/by/4.0/).